Fast-timing lifetime measurement of ^{152}Gd

J. Wiederhold,[1,*] R. Kern,[1] C. Lizarazo,[1] N. Pietralla,[1] V. Werner,[1] R. V. Jolos,[2,3] D. Bucurescu,[4] N. Florea,[4] D. Ghita,[4] T. Glodariu,[4] R. Lica,[4] N. Marginean,[4] R. Marginean,[4] C. Mihai,[4] R. Mihai,[4] I. O. Mitu,[4] A. Negret,[4] C. Nita,[4] A. Olacel,[4] S. Pascu,[4] L. Stroe,[4] S. Toma,[4] and A. Turturica[4]

[1]*Institut für Kernphysik Technische Universität Darmstadt, Schlossgartenstraße 9 64289 Darmstadt, Germany*

[2]*Joint Institute for Nuclear Research, Dubna, Moscow Oblast 141980, Russia*

[3]*Dubna State University, Dubna, Moscow Oblast 141980, Russia*

[4]*"Horia Hulubei" National Institute for Physics and Nuclear Engineering, 077125 Bucharest-Magurele, Romania*

(Received 8 August 2016; published 3 October 2016)

The lifetime $\tau(0_2^+)$ of ^{152}Gd has been measured using fast electronic scintillation timing (FEST) with an array of high-purity germanium (HPGe) and cerium-doped lanthanum bromide ($LaBr_3$) detectors. ^{152}Gd was produced via an (α,n) reaction on a gold backed ^{149}Sm target. The measured lifetime of $\tau(0_2^+) = 96(6)$ ps corresponds to a reduced transition strength of $B(E2;0_2^+ \rightarrow 2_1^+) = 111(7)$ W.u. and an $E0$ transition strength of $\rho^2(E0) = 39(3) \times 10^{-3}$ to the ground state. This result provides experimental support for the validity of a correlation that would be a novel indicator for a quantum phase transition (QPT).

DOI: 10.1103/PhysRevC.94.044302

I. INTRODUCTION

Atomic nuclei are complex quantum objects due to interactions of nucleons through complex nuclear forces. Nuclei can appear in various shapes due to collective correlations. Depending on shell structure they can undergo rather rapid shape changes as a function of nucleon number. Well-known examples are found in the Sr, Zr region [1–3] or in the rare-earth region around $N = 90$ [4–11]. In the rare-earth region accessible nuclei range from the closed neutron shell at $N = 82$ to strongly deformed nuclei and have been studied extensively. Empirical signatures for shape changes in a sequence of even-even nuclei are, e.g., a rise in the ratio $R_{4/2} = E(4_1^+)/E(2_1^+)$ or in the easier-to-obtain inverse excitation energy of the first 2^+ state, $1/E(2_1^+)$, the occurrence of a local increase in the two-neutron separation energy S_{2n}, and a sudden rise in the $E2$ transition strength $B(E2;2_1^+ \rightarrow 0_{gs}^+)$ or the ratio $E(6_1^+)/E(0_2^+)$ [12]. Figure 1 shows selected observables for the Sm and Gd isotopes, that clearly indicate a quantum phase transition (QPT) around $N = 90$.

For a better understanding of the phenomenon of nuclear shape transitions, it is of interest to study the correlation of these observables [24–26], or to establish links to other observables that indicate changes in structure.

Another signature for a QPT is the $E0$-transition strength $\rho^2(E0)$. In the framework of the interacting boson model (IBM) [27] it could be shown that $\rho^2(E0)$ sharply increases in spherical-deformed shape transition regions [28] and maximizes but may remain sizable in deformed nuclei. In the confined β soft (CBS) rotor model [29] it was shown that $\rho^2(E0)$ should decrease from the transitional region toward the rigid rotor limit [30].

The $E0$ transition rate is defined as [31]

$$\rho^2_{if}(E0) = \frac{|\langle \Psi_f|\hat{T}(E0)|\Psi_i\rangle|^2}{(eR^2)^2}. \tag{1}$$

The $E0$ transition operator [30]

$$\hat{T}(E0) = \frac{3Z}{4\pi} eR^2\hat{\beta}^2 \tag{2}$$

is related to the $E2$ transition operator

$$\hat{T}(E2) = \frac{3Z}{4\pi} eR^2\hat{\beta}, \tag{3}$$

with the nuclear radius $R = 1.2 \times A^{1/3}$ fm and the deformation parameter operator $\hat{\beta}$. The $E0$ transition rate between the first and the ith 0^+-state is given by

$$\rho_i^2(E0) = \left(\frac{3Z}{4\pi}\right)^2 |\langle 0_1^+|\hat{\beta}^2|0_i^+\rangle|^2, \tag{4}$$

$$= \left(\frac{3Z}{4\pi}\right)^2 |\Sigma_j \langle 0_1^+|\hat{\beta}|2_j^+\rangle\langle 2_j^+|\hat{\beta}|0_i^+\rangle|^2, \tag{5}$$

where the total $E0$ transition strength to the ground state is typically exhausted by the first two excited 0^+ states [28], hence, in this work i is 2 or 3. For even-even nuclei, the Q-phonon approach was developed [32–37] to approximate collective low-lying positive-parity states in terms of multiple quadrupole (Q) phonon excitations of the ground state $|0_1^+\rangle$:

$$|L^+,n\rangle = N^{(L,n)}(\underbrace{Q\cdots Q}_{n})^{(L)}|0_1^+\rangle.$$

It was shown that the 2_1^+ state of all collective even nuclei from $Z = 30$ to 100 nearly exhaust the known $E2$ strength from the ground state [34] with some deviations in the vibrator-to-rotor transition region. In this approximation, and identifying the

*jwiederhold@ikp.tu-darmstadt.de

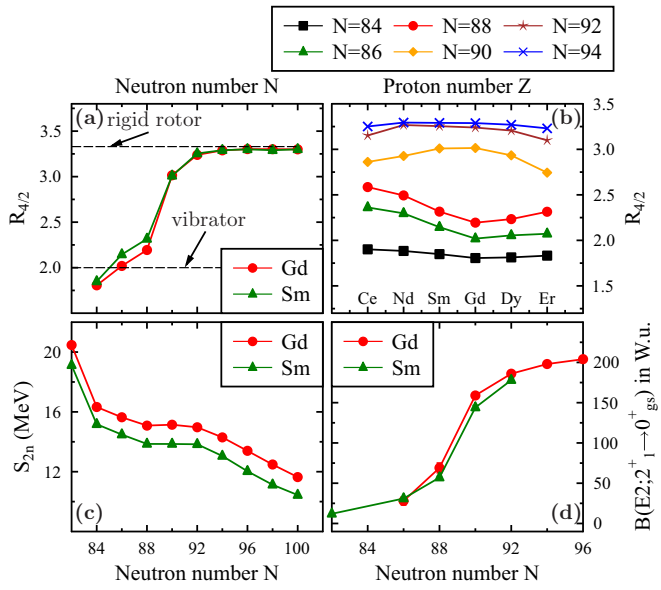

FIG. 1. (a) The $R_{4/2}$ ratio for the Gd and Sm isotopes around $N = 90$. A sudden rise in the ratio is visible between $N = 88$ and $N = 90$. (b) $R_{4/2}$ vs proton number for $N = 84$ to $N = 94$. The gap between $N = 88$ and $N = 90$ increases up to $Z = 64$ [13]. (c) Two-neutron separation energy S_{2n} vs neutron number N for Sm and Gd isotopes. (d) $B(E2; 2^+_1 \rightarrow 0^+_{gs})$ vs neutron number. Data were taken from the Nuclear Data Sheets [14–23].

quadrupole operator Q with the $E2$ transition operator, one obtains

$$\rho^2(E0) \approx \left(\frac{3Z}{4\pi}\right)^2 |\langle 0^+_1|\hat{\beta}|2^+_1\rangle\langle 2^+_1|\hat{\beta}|0^+_2\rangle|^2, \tag{6}$$

$$= \left(\frac{4\pi}{3Z}\right)^2 \frac{5}{(eR^2)^4} B(E2; 0^+_2 \rightarrow 2^+_1) B(E2; 2^+_1 \rightarrow 0^+_1), \tag{7}$$

$$\equiv \left(\frac{4\pi}{3Z}\right)^2 \frac{5}{(eR^2)^4} B(E2)_2 B(E2)_1. \tag{8}$$

Figure 2 shows the literature data on $\rho^2(E0)$, the left-hand side (lhs) of Eq. (8) and the product of $B(E2)$ values, the right-hand side (rhs) of Eq. (8) for the gadolinium and samarium isotopes around $N = 90$. The data, indeed, show a correlation with respect to a decrease with neutron number beyond $N = 90$. In $^{152-156}$Gd the 0^+_2 state dominates the known $E0$ strength from the ground state. Note that in ^{158}Gd the 0^+_3 state carries a sizable $E0$ strength to the ground state, which, however, is smaller than $\rho^2(E0; 0^+_2 \rightarrow 0^+_1)$ of ^{156}Gd. For completeness, this value is included in Figs. 2 and 6. Moreover, the $\rho^2(E0)$ values in both isotopic chains and the product of $B(E2)$ values in the Sm chain peak at $N = 90$. For ^{152}Gd this expected correlation seems to be invalid. Noteworthy is the big uncertainty for the $B(E2)$ product of ^{152}Gd. This uncertainty stems mainly from the literature value of the lifetime $\tau(0^+_2)$ of ^{152}Gd. There is only one known recoil distance Doppler shift measurement of this lifetime [39]. Implying an unusually large $E2$ decay strength of $B(E2)_2 = 178(54)$ W.u. in this vibrational nucleus casts

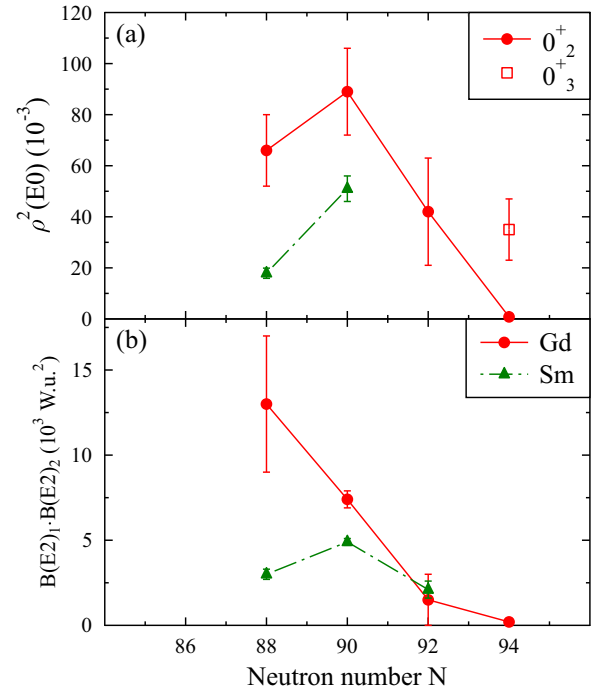

FIG. 2. (a) The $E0$ transition rate $\rho^2(E0)$ for the Gd and Sm isotopes around $N = 90$. For ^{158}Gd also the $\rho^2(E0; 0^+_3 \rightarrow 0^+_{gs})$ transition strength is given. See text. (b) Product $B(E2)_1 \times B(E2)_2$ over neutron number for the Gd and Sm isotopes. Data were taken from the Nuclear Data Sheets [14–23] and [31,38].

doubts on this measurement. In that work it is mentioned, indeed, that the statistics for the measurement were not adequate for an accurate lifetime determination by the standard analysis and it was necessary to sum up data from different target-stopper distances. To renew and eventually improve this value a FEST experiment at the 9 MV Tandem accelerator at the National Institute of Physics and Nuclear Engineering (IFIN-HH) in Bucharest has been carried out.

II. EXPERIMENT AND ANALYSIS

Excited states of ^{152}Gd were populated via the ^{149}Sm$(\alpha,n)^{152}$Gd reaction. To prevent getting contributions from other reaction channels, the beam energy was set to 17.5 MeV, close to the Coulomb barrier for this reaction of 17.18 MeV. The α beam from the Bucharest FN Tandem accelerator impinged on a 1.3 mg/cm^2 thick ^{149}Sm target with 4.3 mg/cm^2 gold backing. The backing was used to stabilize the target. The enrichment of the target was 93.2% of ^{149}Sm with small contaminations from ^{150}Sm (3.3%), ^{148}Sm (1.5%), ^{152}Sm (1.2%) and 0.8% of other isotopes. The experiment ran for about 180 hours with an average beam intensity of 30 nA. Deexcitation γ rays were detected using the Rosphere detector array in a configuration with 11 $LaBr_3$ and 14 high-purity germanium (HPGe) detectors [40], that are arranged in five rings around the target chamber. The master-trigger condition for the experiment was either two or more coincident γ rays in the $LaBr_3$ detectors or two or more coincident γ rays in the HPGe detectors. Also down-scaled singles events in the

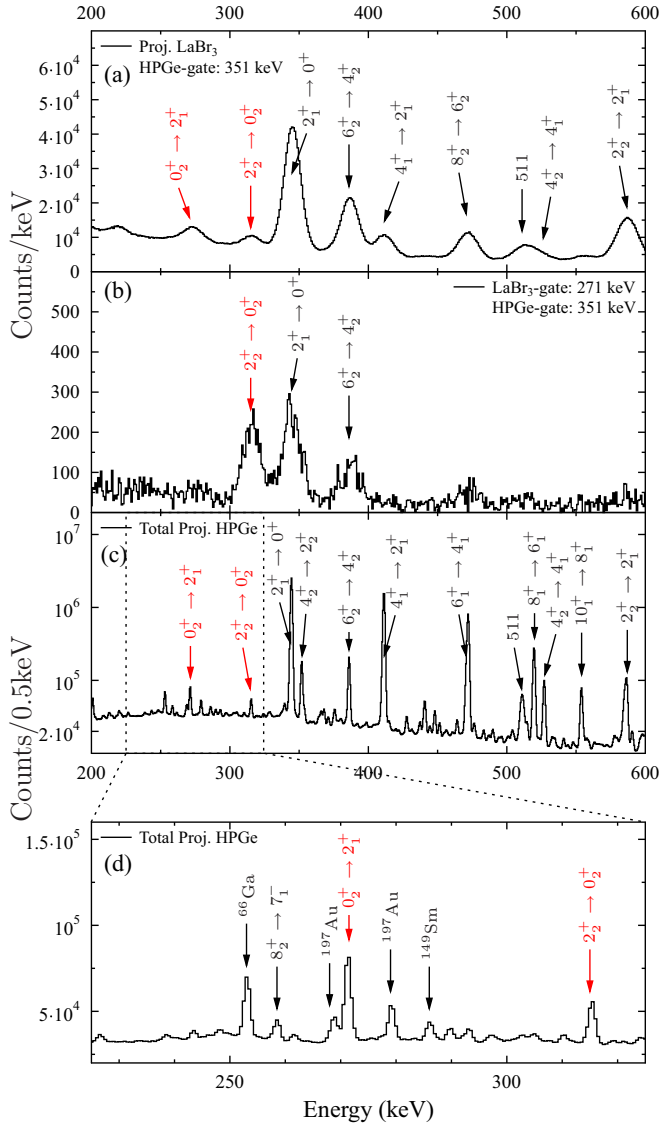

FIG. 3. (a) Energy projection of a $E_{\mathrm{LaBr_3}}$-$E_{\mathrm{LaBr_3}}$-Δt cube in the energy range from 200 to 600 keV. An additional gate was set in the HPGe detectors on the $4_2^+ \rightarrow 2_2^+$ transition at 351 keV. Marked red are the important transitions to determine $\tau(0_2^+)$. (b) Coincidence spectrum gated on the 271 keV $0_2^+ \rightarrow 2_1^+$ transition in spectrum (a). (c) Total projection of the E_{HPGe}-E_{HPGe} matrix. (d) Zoom-in on the region of interest between 225 and 325 keV.

HPGe detectors were recorded. The energy calibration was done using a ^{152}Eu source, which also was used to determine the energy-dependent time walk of the experimental setup.

A. Spectroscopy

Because of the clean reaction channel the γ-ray transitions of ^{152}Gd could be clearly identified using the HPGe detectors with an energy resolution of about 3 keV at 1.4 MeV and 2.5 keV at 300 keV. Figure 3(c) shows the total projection of the HPGe-detector coincidence matrix between 200 and 600 keV. Clearly visible are the yrast transitions up to the $10_1^+ \rightarrow 8_1^+$ transition. Furthermore, many other transitions can be resolved. Figure 3(d) shows the energy spectra zoomed in on the relevant transitions to determine the lifetime of the 0_2^+ state. There are nearly no contaminations of other reactions visible, only some small contributions from Coulomb excitation of the beam with the target backing or (α,n) reactions with Cu parts in the target chamber. To eliminate contributions of these contaminations, additional gates were set in the HPGe detectors excluding these transitions in the gates on the energy of the $LaBr_3$ detectors. For example, the Au transitions near the $0_2^+ \rightarrow 2_2^+$ transition at 271 keV cannot be separated in the $LaBr_3$ detectors; see Fig. 3(d). Figure 3(a) shows the energy projection of the $LaBr_3$-detector coincidence matrix in coincidence with the 351 keV ($4_2^+ \rightarrow 2_2^+$) transition observed in the HPGe detectors. Figure 3(b) shows the $LaBr_3$ coincidence spectrum gated in addition on the transition $0_2^+ \rightarrow 2_1^+$ at 271 keV. After having set these gates, there are no contaminations visible in the $LaBr_3$ energy spectra and clean gates can be set on the relevant transitions to analyze the corresponding time differences for determining the lifetime of the 0_2^+ state.

B. Time walk

In fast-timing measurements, the lifetime is determined by measuring the time difference between a start and a stop signal. For the lifetime of an excited state in a nucleus, two γ-ray transitions, one that feeds the state and a decay transition, can be used as start and stop signals or vice versa for a time-to-amplitude converter (TAC). A more detailed description of the setup and the fast-timing method is given in [41–43]. Time walk as a function of transition energy is generated by differences in the amplitude or the rise time of the input signals in the constant-fraction discriminators (CFDs) and the detector geometry. When measuring the time differences between γ-ray transitions, the measured times are equal to the effective lifetime of the nuclear states: the sum of the lifetimes [41] that lie between the γ-ray transitions and the energy-dependent time walk of both signals,

$$\Delta t = \tau_{\mathrm{eff}} + t_{\text{time-walk},1}(E_{\gamma,1}) + t_{\text{time-walk},2}(E_{\gamma,2}). \qquad (9)$$

So only the sum of the time walk for a combination of γ rays can be measured. To determine the lifetime, the energy-dependent time walk of every detector was determined using an ^{152}Eu source with its well known γ lines from ^{152}Gd and ^{152}Sm ranging from 244 to 1299 keV (see Fig. 4), as described in [44] by fitting a polynomial function to the time response of every detector and using only the full energy peaks of the Eu source.

After correcting for the time walk to measure the lifetime of excited states, an energy-energy-Δt cube was sorted for the $LaBr_3$ detectors. By selecting the region of the pair of coincident γ rays (e.g., 271 and 315 keV for the 0_2^+ state) in the energy-energy plane of this cube a time difference spectrum can be extracted. A correction for random coincidences and the Compton background was done by selecting an area near the peak in the energy-energy plane. By subtracting the background time-difference spectrum, normalized to the peak time-difference spectrum, from the peak spectrum, a

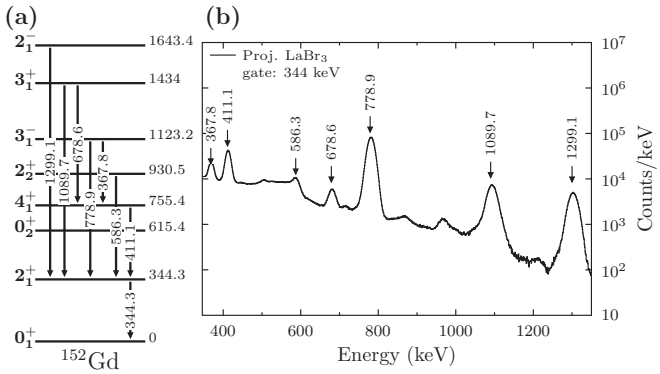

FIG. 4. (a) Partial level scheme of ^{152}Gd after β^- decay of ^{152}Eu. (b) Coincidence γ-ray spectrum for the $LaBr_3$ detectors obtained by gating on the $2_1^+ \rightarrow 0_{gs}^+$ transition at 344 keV of ^{152}Gd after β^- decay of ^{152}Eu.

background-subtracted time-difference spectrum for the pair of coincidences was established.

The typical delayed time distribution, assuming there are no background contributions, is a convolution of the prompt response function (PRF) of the setup, $P(t')$, and the exponential decay [45]:

$$D_\lambda(t) = n\lambda \int_{-\infty}^{t} P(t')e^{-\lambda(t-t')}dt', \tag{10}$$

with the transition rate $\lambda = 1/\tau$ and the normalization n. The centroid of the time-distribution is defined as [41,46]

$$C(D_\lambda) = \langle t \rangle = \frac{\int t D_\lambda(t)dt}{\int D_\lambda(t)dt}, \tag{11}$$

resulting in

$$\tau = C(D_\lambda) - C(P), \tag{12}$$

with the centroid of the delayed time distribution $C(D_\lambda)$ and the centroid of the prompt response $C(P)$, which is just the centroid of $P(t')$. This equation is valid for the case that the start-gate is set on the feeding transition. When the gates are switched also $C(D_\lambda)$ and $C(P)$ switch places in the equation. It follows, for the centroid difference [47],

$$\Delta C = C(D_\lambda)_{\text{Stop}} - C(D_\lambda)_{\text{Start}} \tag{13}$$

$$= C(P)_{\text{Stop}} + \tau - [C(P)_{\text{Start}} - \tau] \tag{14}$$

$$= 2\tau. \tag{15}$$

After the time-walk correction, $C(P)_{\text{Stop}}$ is equal to $C(P)_{\text{Start}}$. With this centroid-difference method, lifetimes below the FWHM of the PRF can be determined. For $LaBr_3$ detectors the FWHM is usually around 100–300 ps, depending on the crystal size. To test the calibrations and corrections, some well known lifetimes of states of ^{152}Gd and the lifetime of the first 2^+ state of ^{152}Sm from the Eu source were determined. The results are listed in Table I. The measured lifetimes of the 2_1^+ and 4_1^+ states of ^{152}Gd were in good agreement with literature values. The value for the 2_1^+ state of ^{152}Sm differs slightly from the adopted value found in [17]. But there are many experiments that are in agreement

TABLE I. Measured Lifetimes of ^{152}Gd and the used start and stop transitions. The centroid difference was determined by comparing the time spectra with switched gates. For the lifetime of the 2_1^+ state of ^{152}Sm the time distribution was fitted using Eq. (10). The quoted error represents the contribution of the statistical error by determining the centroids or the fit and the uncertainty of the time-walk distribution.

Nucleus	J_n^p	Gate 1	Gate 2	$\tau = \Delta C/2$ (ps)	$\tau_{\text{lit.}}$[a] (ps)
^{152}Gd	2_1^+	$4_1^+ \rightarrow 2_1^+$	$2_1^+ \rightarrow 0_1^+$	51(6)	46(4)
	2_1^+	$2_2^+ \rightarrow 2_1^+$	$2_1^+ \rightarrow 0_1^+$	46(6)	46(4)
	4_1^+	$6_1^+ \rightarrow 4_1^+$	$4_1^+ \rightarrow 2_1^+$	9(6)	11(1)
	0_2^+	$0_2^+ \rightarrow 2_1^+$	$2_2^+ \rightarrow 0_2^+$	96(6)	53(12)
^{152}Sm	2_1^+	$4_1^+ \rightarrow 2_1^+$	$2_1^+ \rightarrow 0_1^+$	2049(10)	2024(16)

[a]Data taken from [17].

with the measured value (e.g., the average value of $\tau(2_1^+)$ from Coulomb excitation experiments is 2.049(17) ns). As mentioned before there are two γ lines coming from the gold backing near the $0_2^+ \rightarrow 2_1^+$ transition at 271 keV. To exclude any contribution from these transitions another gate was set in the HPGe detectors to select the right decay cascade of ^{152}Gd. In Fig. 5 (top panel) the gate was set on the transition $2_1^+ \rightarrow 0_{gs}^+$ at 344 keV and (bottom panel) on the transition $4_2^+ \rightarrow 2_2^+$ at 351 keV. Both obtained lifetime values agree well

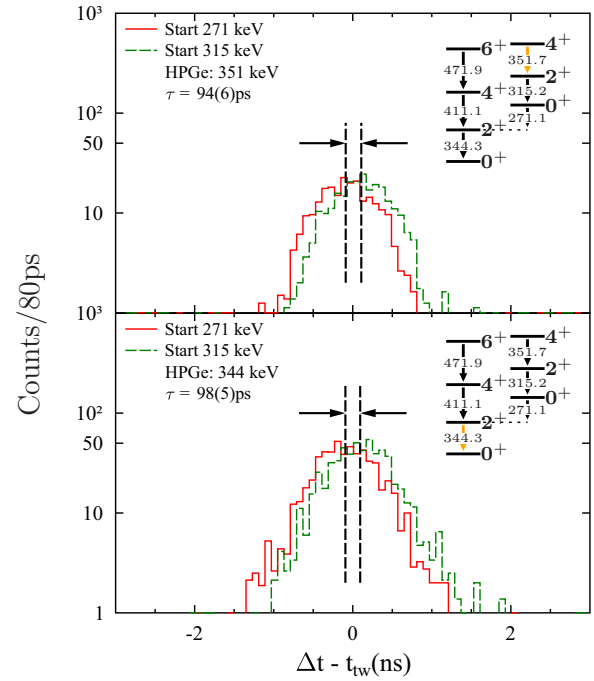

FIG. 5. Top: Time-difference spectra for the combination of start gate on 315 keV ($2_2^+ \rightarrow 0_2^+$) and stop gate on 271 keV ($0_2^+ \rightarrow 2_1^+$) in green (dashed line) and vice versa in red with an additional gate on 344 keV ($2_1^+ \rightarrow 0_{gs}^+$) in the HPGe detectors. Bottom: The same with a different gate for the HPGe detectors ($4_2^+ \rightarrow 2_2^+$ at 351 keV). The right top corner shows a partial level scheme of ^{152}Gd. Marked in orange is the HPGe gate.

and the average of the lifetime $\tau(0_2^+)$ of ^{152}Gd was determined to be 96(6) ps or $T_{1/2} = 67(4)$ ps.

III. DISCUSSION

After determining the new value for the lifetime $\tau(0_2^+)$ it is possible to calculate the $E2$ transition strength with the conversion coefficient $\alpha = 0.0826(12)$ from Ref. [48]:

$$B(E2; 0_2^+ \rightarrow 2_1^+) = 0.536(33)\ e^2b^2, \\ = 111(7)\ \text{W.u.} \qquad (16)$$

The quoted error represents the statistical error in determining the centroids and the contributions to the error from the energy-dependent time walk. In addition, from this new value of the $B(E2; 0_2^+ \rightarrow 2_1^+)$ strength a new value for the $\rho^2(E0)$ transition strength can be determined using the dimensionless ratio of the $E0$ and $E2$ transitions defined by Rasmussen [49]:

$$X(E0/E2) \equiv \frac{B(E0)}{B(E2)} = \frac{\rho^2(E0)e^2R^4}{B(E2)}. \qquad (17)$$

With the measured value of $X(E0/E2) = 0.0122(5)$ given in Ref. [38] and the newly determined $B(E2; 0_2^+ \rightarrow 2_1^+)$ value one obtains

$$\rho^2(E0) = 39(3)\times10^{-3}. \qquad (18)$$

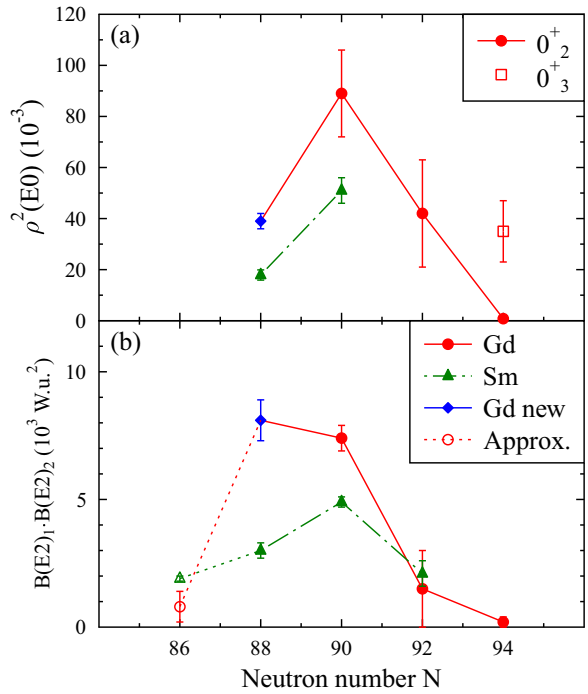

FIG. 6. (a) Experimental values of $\rho^2(E0)$ values for the $0_2^+ \rightarrow 0_1^+$ transition for Gd and Sm isotopes. Blue (filled diamond) value from this work. For ^{158}Gd the $\rho^2(E0; 0_3^+ \rightarrow 0_1^+)$ value is shown, too. See text. (b) Product $B(E2)_1B(E2)_2$ of Gd and Sm isotopes. Blue (filled diamond) value from this work. For $N = 86$ isotopes, there is no lifetime data of the 0_2^+ state. Product $B(E2)_1B(E2)_2$ was approximated; see text. Data taken from Table II.

TABLE II. $B(E2)_i$ transition strengths of even-even Gd and Sm isotopes around $N = 90$ (^{154}Gd,^{152}Sm). $B(E2)$ values were calculated using the literature values of $\tau(0_2^+,2_1^+)$, α, and E_γ. In addition the literature values for the $E0$ transition strength $\rho^2(E0)$ are shown. Data were taken from [15–20].

Isotope	$B(E2)_1$ (W.u.)	$B(E2)_2$ (W.u.)	$B(E2)_1 \times B(E2)_2$ (10^3 W.u.^{2})	$\rho_i^2(E0)$ (10^{-3})[a]
^{146}Gd	$\geqslant$0.6		$\geqslant$0.001[b]	7.2(9)
^{148}Gd	10(3)		0.2(1)[b]	
^{150}Gd	20(8)[c]		0.8(6)[b]	
^{152}Gd	73(6)	111(7)[d]	8.1(8)[d]	39(3)[d]
^{154}Gd	157(3)	47(3)	7.4(5)	89(17)
^{156}Gd	188(3)	8(8)	1.5(15)	42(21)
^{158}Gd	201(4)	1.2(8)	0.2(2)	$\leqslant$0.08 35(12)[e]
^{148}Sm	31(1)		1.9(1)[b]	
^{150}Sm	56(2)	53(5)	3.0(3)	17.9(20)
^{152}Sm	145(2)	34(1)	4.9(2)	51(5)
^{154}Sm	176(3)	12(3)	2.1(5)	

[a]Taken from [31,38].
[b]Approximation using Eq. (21).
[c]Taken from S. Pascu (unpublished).
[d]From this work.
[e]Given is $\rho^2(E0; 0_3^+ \rightarrow 0_{gs}^+)$.

Figure 6 shows the $E0$ strength $\rho^2(E0)$ and the product $B(E2)_1 \times B(E2)_2$ over the neutron number which are also listed in Table II. The maximum at $N = 90$ for $\rho^2(E0)$ with the new data point is more pronounced and the uncertainty has been reduced significantly. Nevertheless the $0_2^+ \rightarrow 0_1^+$ $E0$ transition strength is considerably large in ^{152}Gd, which supports the argument that ^{152}Gd lies already near the QPT. For the product of $B(E2)$ values the maximum lies between $N = 88$ and $N = 90$. It does not exactly coincide with the location of the maximum of the $E0$ strength. This may be traced back to the approximation of the applied Q-phonon scheme.

In general the $B(E2)$ product is expected to maximize in the transitional region, which can also qualitatively be shown in the context of the geometrical Davydov-Chaban model [50] and the vibrational model. Using the intrinsic frame expression for the $E2$-transition operator

$$Q_{2\mu} = Q_0 D^2_{\mu 0}\beta, \qquad (19)$$

results, for the product of $B(E2)$ transition strengths, in

$$B(E2; 0_1^+ \rightarrow 2_1^+)B(E2; 0_2^+ \rightarrow 2_1^+) = Q_0^4|\langle 0_1^+|\beta^2|0_2^+\rangle|^2. \qquad (20)$$

With wave functions obtained from the Davydov-Chaban and vibrator models and typical values for the deformation β and the fluctuation of the deformation, it can be shown, that there should be a maximum for the $B(E2)$ product for transitional nuclei featuring both substantial deformation and maximum fluctuation.

Since for vibrator models $B(E2; 0_2^+ \rightarrow 2_1^+) = 2 \times B(E2; 2_1^+ \rightarrow 0_1^+)$, one can estimate a reasonable upper

limit

$$B(E2)_1 B(E2)_2 = 2[B(E2)_1]^2, \quad (21)$$

for vibrational nuclei such as ^{150}Gd and ^{148}Sm, which were included in Fig. 6. Using this approximation shows that the product of $B(E2)$ values goes to small values for nuclei below the QPT [see Fig. 6(b)] and there is indeed a maximum at or between $N = 88$ and $N = 90$.

IV. SUMMARY

Lifetimes of ^{152}Gd were measured using the fast-timing technique. The known lifetimes of the 2_1^+ and 4_1^+ states could be confirmed. The measured lifetime of the 0_2^+ state, 96(6) ps is nearly two times the previously measured one, 53(12) ps [39]. With the new value for $\tau(0_2^+)$ of ^{152}Gd the $\rho^2(E0)$ transition strength could be determined to $39(3) \times 10^{-3}$ and the $B(E2; 0_2^+ \rightarrow 2_1^+)$ transition strength to 0.536(33) e^2b^2 or 111(7) W.u.

The $\rho^2(E0)$ values for the 0_2^+ state and the absolute strength product of the $E2$-$E2$ cascade, $B(E2)_2 B(E2)_1$, peak at $N = 90$ or between $N = 88$ and $N = 90$, indicating a QPT.

ACKNOWLEDGMENTS

The authors thank the tandem accelerator crew for their support during the experiment. This work was supported by the Deutsche Forschungsgemeinschaft under Grant No. SFB 634 and the BMBF under Grant No. 05P15RDFN9 within the collaboration 05P15 NuSTAR R&D.

[1] E. Cheifetz, R. C. Jared, S. G. Thompson, and J. B. Wilhelmy, Phys. Rev. Lett. **25**, 38 (1970).
[2] P. Federman and S. Pittel, Phys. Lett. B **69**, 385 (1977).
[3] C. Kremer, S. Aslanidou, S. Bassauer, M. Hilcker, A. Krugmann, P. von Neumann-Cosel, T. Otsuka, N. Pietralla, V. Y. Ponomarev, N. Shimizu, M. Singer, G. Steinhilber, T. Togashi, Y. Tsunoda, V. Werner, and M. Zweidinger [Phys. Rev. Lett. (to be published)], arXiv:1606.09057.
[4] R. F. Casten, D. D. Warner, D. S. Brenner, and R. L. Gill, Phys. Rev. Lett. **47**, 1433 (1981).
[5] F. Iachello, Phys. Rev. Lett. **87**, 052502 (2001).
[6] R. F. Casten and N. V. Zamfir, Phys. Rev. Lett. **87**, 052503 (2001).
[7] R. Krücken, B. Albanna, C. Bialik, R. F. Casten, J. R. Cooper, A. Dewald, N. V. Zamfir, C. J. Barton, C. W. Beausang, M. A. Caprio, A. A. Hecht, T. Klug, J. R. Novak, N. Pietralla, and P. von Brentano, Phys. Rev. Lett. **88**, 232501 (2002).
[8] D. Tonev, A. Dewald, T. Klug, P. Petkov, J. Jolie, A. Fitzler, O. Möller, S. Heinze, P. von Brentano, and R. F. Casten, Phys. Rev. C **69**, 034334 (2004).
[9] D. A. Meyer, V. Wood, R. F. Casten, C. R. Fitzpatrick, G. Graw, D. Bucurescu, J. Jolie, P. von Brentano, R. Hertenberger, H.-F. Wirth, N. Braun, T. Faestermann, S. Heinze, J. L. Jerke, R. Krücken, M. Mahgoub, O. Möller, D. Mücher, and C. Scholl, Phys. Rev. C **74**, 044309 (2006).
[10] V. Werner, E. Williams, R. J. Casperson, R. F. Casten, C. Scholl, and P. von Brentano, Phys. Rev. C **78**, 051303 (2008).
[11] R. V. Jolos and P. von Brentano, Phys. Rev. C **80**, 034308 (2009).
[12] D. Bonatsos, E. A. McCutchan, R. F. Casten, and R. J. Casperson, Phys. Rev. Lett. **100**, 142501 (2008).
[13] R. B. Cakirli and R. F. Casten, Phys. Rev. C **78**, 041301 (2008).
[14] L. K. Peker and J. K. Tuli, Nucl. Data Sheets **82**, 187 (1997).
[15] N. Nica, Nucl. Data Sheets **117**, 1 (2014).
[16] S. K. Basu and A. A. Sonzogni, Nucl. Data Sheets **114**, 435 (2013).
[17] M. J. Martin, Nucl. Data Sheets **114**, 1497 (2013).
[18] C. W. Reich, Nucl. Data Sheets **110**, 2257 (2009).
[19] C. W. Reich, Nucl. Data Sheets **113**, 2537 (2012).
[20] R. G. Helmer, Nucl. Data Sheets **101**, 325 (2004).
[21] C. W. Reich, Nucl. Data Sheets **105**, 557 (2005).
[22] C. W. Reich, Nucl. Data Sheets **108**, 1807 (2007).
[23] B. Singh, Nucl. Data Sheets **93**, 243 (2001).
[24] R. F. Casten, Prog. Part. Nucl. Phys. **62**, 183 (2009).
[25] P. Cejnar and J. Jolie, Prog. Part. Nucl. Phys. **62**, 210 (2009).
[26] E. A. McCutchan, N. V. Zamfir, and R. F. Casten, Phys. Rev. C **69**, 064306 (2004).
[27] F. Iachello and A. Arima, *The Interacting Boson Model* (Cambridge University Press, 2006).
[28] P. von Brentano, V. Werner, R. F. Casten, C. Scholl, E. A. McCutchan, R. Krucken, and J. Jolie, Phys. Rev. Lett. **93**, 152502 (2004).
[29] N. Pietralla and O. M. Gorbachenko, Phys. Rev. C **70**, 011304 (2004).
[30] J. Bonnet, A. Krugmann, J. Beller, N. Pietralla, and R. V. Jolos, Phys. Rev. C **79**, 034307 (2009).
[31] J. L. Wood, E. F. Zganjar, C. De Coster, and K. Heyde, Nucl. Phys. A **651**, 323 (1999).
[32] G. Siems, U. Neuneyer, I. Wiedenhöver, S. Albers, M. Eschenauer, R. Wirowski, A. Gelberg, P. von Brentano, and T. Otsuka, Phys. Lett. B **320**, 1 (1994).
[33] T. Otsuka and K.-H. Kim, Phys. Rev. C **50**, R1768 (1994).
[34] N. Pietralla, P. von Brentano, R. F. Casten, T. Otsuka, and N. V. Zamfir, Phys. Rev. Lett. **73**, 2962 (1994).
[35] N. Pietralla, P. von Brentano, T. Otsuka, and R. F. Casten, Phys. Lett. B **349**, 1 (1995).
[36] N. Pietralla, T. Mizusaki, P. von Brentano, R. V. Jolos, T. Otsuka, and V. Werner, Phys. Rev. C **57**, 150 (1998).
[37] Y. V. Palchikov, P. von Brentano, and R. V. Jolos, Phys. Rev. C **57**, 3026 (1998).
[38] T. Kibédi and R. H. Spear, At. Data Nucl. Data Tables **89**, 77 (2005).
[39] N. R. Johnson, I. Y. Lee, F. K. McGowan, T. T. Sugihara, S. W. Yates, and M. W. Guidry, Phys. Rev. C **26**, 1004 (1982).
[40] D. Bucurescu *et al.* (unpublished).
[41] H. Mach, R. L. Gill, and M. Moszyński, Nucl. Instrum. Methods Phys. Res., Sect. A **280**, 49 (1989).
[42] M. Moszyński and H. Mach, Nucl. Instrum. Methods Phys. Res., Sect. A **277**, 407 (1989).
[43] J.-M. Régis, H. Mach, G. S. Simpson, J. Jolie, G. Pascovici, N. Saed-Samii, N. Warr, A. Bruce, J. Degenkolb, L. M. Fraile, C. Fransen, D. G. Ghita, S. Kisyov, U. Koester, A. Korgul, S. Lalkovski, N. Mărginean, P. Mutti, B. Olaizola, Z. Podolyak,

P. H. Regan, O. J. Roberts, M. Rudigier, L. Stroe, W. Urban, and D. Wilmsen, Nucl. Instrum. Methods Phys. Res., Sect. A **726**, 191 (2013).

[44] N. Mărginean, D. L. Balabanski, D. Bucurescu, S. Lalkovski, L. Atanasova, G. Căta-Danil, I. Căta-Danil, J. M. Daugas, D. Deleanu, P. Detistov, G. Deyanova, D. Filipescu, G. Georgiev, D. Ghită, K. A. Gladnishki, R. Lozeva, T. Glodariu, M. Ivaşcu, S. Kisyov, C. Mihai, R. Mărginean, A. Negret, S. Pascu, D. Radulov, T. Sava, L. Stroe, G. Suliman, and N. V. Zamfir, Eur. Phys. J. A **46**, 329 (2010).

[45] L. Boström, B. Olsen, W. Schneider, and E. Matthias, Nucl. Instrum. Methods **44**, 61 (1966).

[46] Z. Bay, Phys. Rev. **77**, 419 (1950).

[47] J.-M. Régis, G. Pascovici, J. Jolie, and M. Rudigier, Nucl. Instrum. Methods Phys. Res., Sect. A **622**, 83 (2010).

[48] T. Kibédi, T. W. Burrows, M. B. Trzhaskovskaya, P. M. Davidson, and C. W. Nestor, Jr., Nucl. Instrum. Methods Phys. Res., Sect. A **589**, 202 (2008).

[49] J. O. Rasmussen, Nucl. Phys. **19**, 85 (1960).

[50] A. S. Davydov and A. A. Chaban, Nucl. Phys. **20**, 499 (1960).